Thalamic extrapontine lesions in central pontine myelinolysis.

T M Koci, F Chiang, P Chow, A Wang, L C Chiu, H Itabashi and C M Mehringer

AJNR Am J Neuroradiol 1990, 11 (6) 1229-1233
http://www.ajnr.org/content/11/6/1229.citation

Thalamic Extrapontine Lesions in Central Pontine Myelinolysis

Timothy M. Koci,[1] Frances Chiang,[1] Peter Chow,[1,2] Angela Wang,[3] Lee C. Chiu,[1,2] Hideo Itabashi,[4] and C. Mark Mehringer[1]

Central pontine myelinolysis (CPM) is a well-known entity first described by Adams et al. in 1959 [1]. This demyelinating disorder is associated with electrolyte disturbances (particularly of sodium) and typically occurs in the setting of alcoholism and malnutrition. Extrapontine myelinolysis (EPM) is identified pathologically in about 53% of cases [2] and, of these, thalamic lesions are detected in 34%.

Recent case reports have described MR findings in EPM of the putamina, caudate nuclei, and midbrain [3–5]. Thalamic lesions were also identified in two case reports of CPM [6, 7].

We present three cases in which symmetric thalamic lesions are demonstrated by MR in CPM/EPM and address the characteristic pattern and location of involvement within the thalami.

Case Reports

Case 1

A 47-year-old female alcoholic was admitted in an obtunded and dehydrated state. The patient was arousable and without focal deficit. Serum sodium was 101 mEq/l and potassium 1.8 mEq/l. By day 7, sodium had been corrected to 133 mEq/l. Cranial CT on day 7 showed only mild cerebral atrophy. The clinical course featured variable levels of consciousness, and on day 13 the patient lapsed into a comatose state with decerebrate posturing. Gradual improvement followed, and by day 30 she was awake at times, with absence of ocular pursuit, and purposeful but markedly weak extremity movement.

MR images of the brain obtained on day 33 showed a trident-shaped pontine lesion characteristic of CPM [8]. Prominent symmetric lesions involved the lateral aspect of the thalami. The lesions did not enhance with contrast material.

At follow-up 6 months later, the patient remains in a nursing home, alert but with slurred speech, unable to ambulate or feed herself.

Case 2

A previously healthy 36-year-old man presented with a 2-week history of persistent diarrhea and complaints of weakness and unsteadiness. Upon neurologic examination he was alert and oriented but unable to ambulate independently. Admission serum sodium of 97 mEq/l was corrected to 135 mEq/l by day 3. By day 4, he was increasingly stuporous, with slurred speech. A cranial CT was interpreted as normal. On day 5, following a generalized seizure, the patient's neurologic status deteriorated to a semicomatose "locked in" state. His eyes were open, but he was unresponsive to questions. The upper extremities were flaccid but slightly flexed at the elbows and wrists without withdrawal to noxious stimuli. Extended lower extremities would manifest flexion withdrawal to noxious stimuli.

MR imaging of the brain on day 8 (Figs. 1A and 1B) showed a small central lesion at the median raphe of the basis pontis. Symmetric areas of abnormality were also seen in the putamina, caudate nuclei, and thalami.

A follow-up MR scan on day 24 (Figs. 1C and 1D) showed progression of central pontine and extrapontine lesions. A T1-weighted MR image (Fig. 1E) showed increased signal within the basal ganglia lesions, suggesting petechial hemorrhage.

At follow-up 3 months later, the patient is able to recognize family members but unable to speak or ambulate.

Case 3

A 34-year-old male alcoholic presented with a 2-week history of vomiting and diarrhea, with difficulty walking and frequent falls. Neurologic examination revealed a lethargic patient with slurred speech and an ataxic gait. Initial serum sodium of 102 mEq/l was corrected over the next 48–72 hr. The patient became slightly more coherent, and on day 6 left the hospital against medical advice and entered a chemical dependency center. He became increasingly somnolent and was referred for a cranial CT examination 14 days after initial admission. CT showed subtle central pontine and bilateral thalamic hypoattenuation. His neurologic condition deteriorated, with difficulty swallowing, absent gag reflex, aphasia, and inappropriate crying, laughter, and moaning. His motor tone was increased but his strength was decreased in all four extremities. MR scans of the brain obtained on day 17 (Figs. 2A and 2B) showed a typical central pontine lesion and bilateral thalamic lesions. Sagittal T2-weighted images (not shown) demonstrated extension of the pontine lesion into the midbrain. A follow-up MR study at 2 months (Fig. 2C) showed a decrease in the size of the thalamic lesions.

The patient gradually improved to near his premorbid state, with residual slurred speech and ataxia.

Received December 20, 1989; revision requested March 20, 1990; revision received May 4, 1990; accepted May 11, 1990.
Presented at the annual meeting of the Western Neuroradiological Society, Pebble Beach, CA, October 1989.
[1] Department of Radiology, Harbor-UCLA Medical Center, 1000 W. Carson St., Torrance, CA 90509. Address reprint requests to T. M. Koci.
[2] Present address: Department of Radiology, St. Joseph's Medical Center, Burbank, CA 91505.
[3] Department of Radiology, Rancho Los Amigos Medical Center, Downey, CA 90242.
[4] Department of Pathology, Harbor-UCLA Medical Center, Torrance, CA 90509.

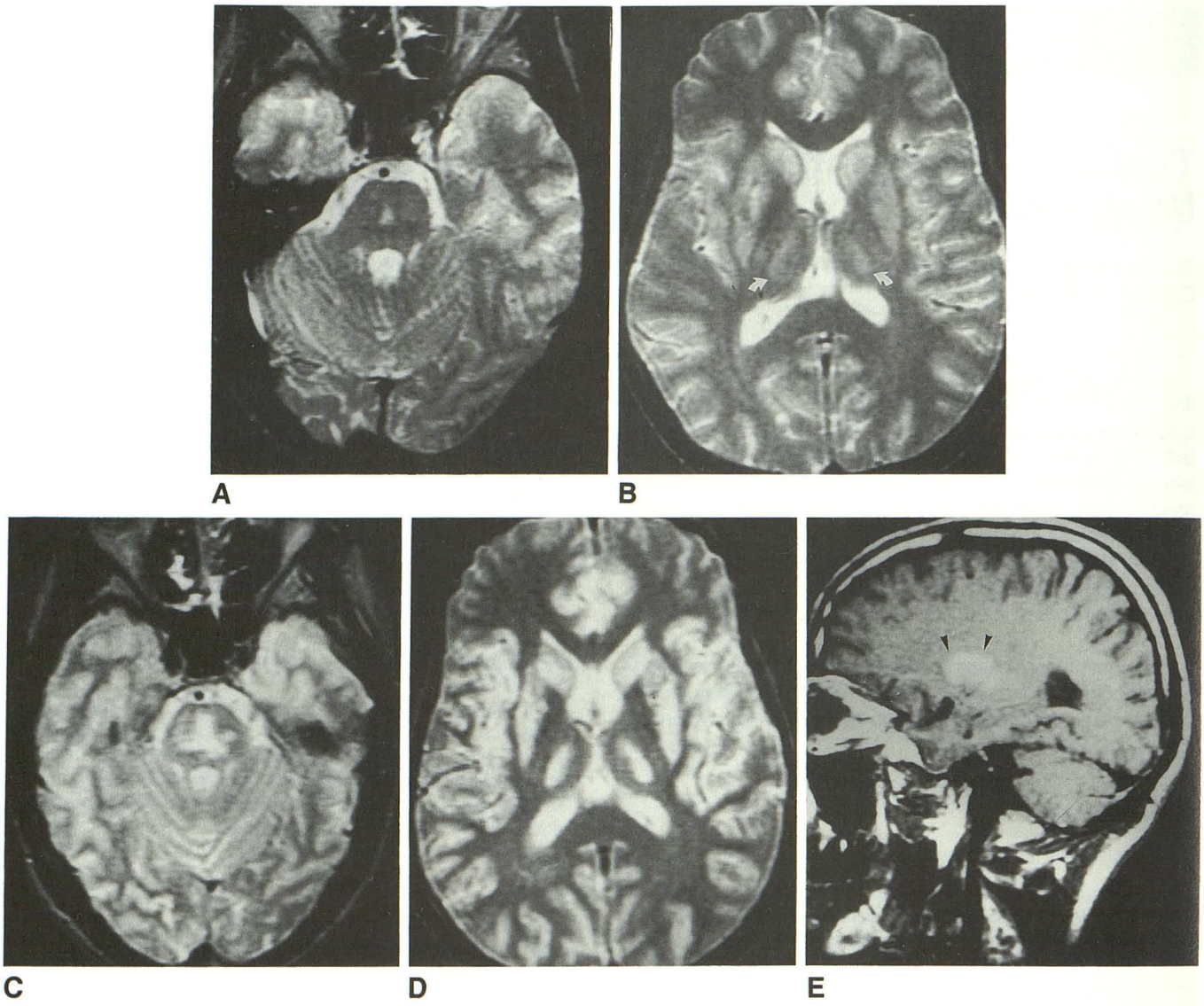

Fig. 1.—Case 2.

A, Axial T2-weighted MR image (2800/80), 8 days after admission shows small hyperintense lesion at median raphe of basis pontis, consistent with early central pontine myelinolysis.

B, Axial T2-weighted MR image (2800/80) on same day shows symmetric areas of high signal in putamina, caudate nuclei, and lateral region of the thalami (*arrows*), consistent with extrapontine myelinolysis.

C and *D*, Axial T2-weighted MR images (2000/80) on day 24. Central pontine lesion (*C*) has become much larger. Image at middorsal thalamic level (*C*) shows interval increase in intensity and definition of putaminal, caudate, and thalamic lesions. Note relative sparing of pulvinar and medial nuclear groups.

E, Parasagittal T1-weighted MR image (617/20) shows hyperintensity in basal ganglia (*arrowheads*), suggesting a hemorrhagic component.

Discussion

The histology, distribution pattern, and frequency of specific extrapontine lesions in CPM have been described in case reports [9–14] and in series [2, 15] described in the neuropathologic literature. In addition to the classic pontine lesions, sites of involvement have been identified microscopically in almost every part of the CNS. In the largest neuropathologic series, Gocht and Colmant [2] studied 58 cases of CPM and/or EPM and reviewed an additional 41 cases from the neuropathologic literature. Pontine lesions were present in 78% and EPM present in 53%. In cases with EPM, histologic lesions were most frequent in the cerebellum (55%), lateral geniculate body (41%), cerebral cortex/subcortex (34%), putamen (34%), and thalamus (34%). Lesions were not graded for severity. Bilateral thalamic lesions were present in two cases of EPM without CPM.

Characteristic patterns of pontine involvement in CPM have been described in the imaging literature [8, 16]. The three cases of EPM presented here would also suggest a tendency for a common if not characteristic pattern of lesion morphology within the thalamus. In reports of thalamic EPM with detailed pathologic study, lateral thalamic involvement predominates, although microscopic involvement in the centromedian, dorsomedial, and intralaminar nuclei also occurs [2, 10–15]. In all three of our cases, there is a similar and distinct

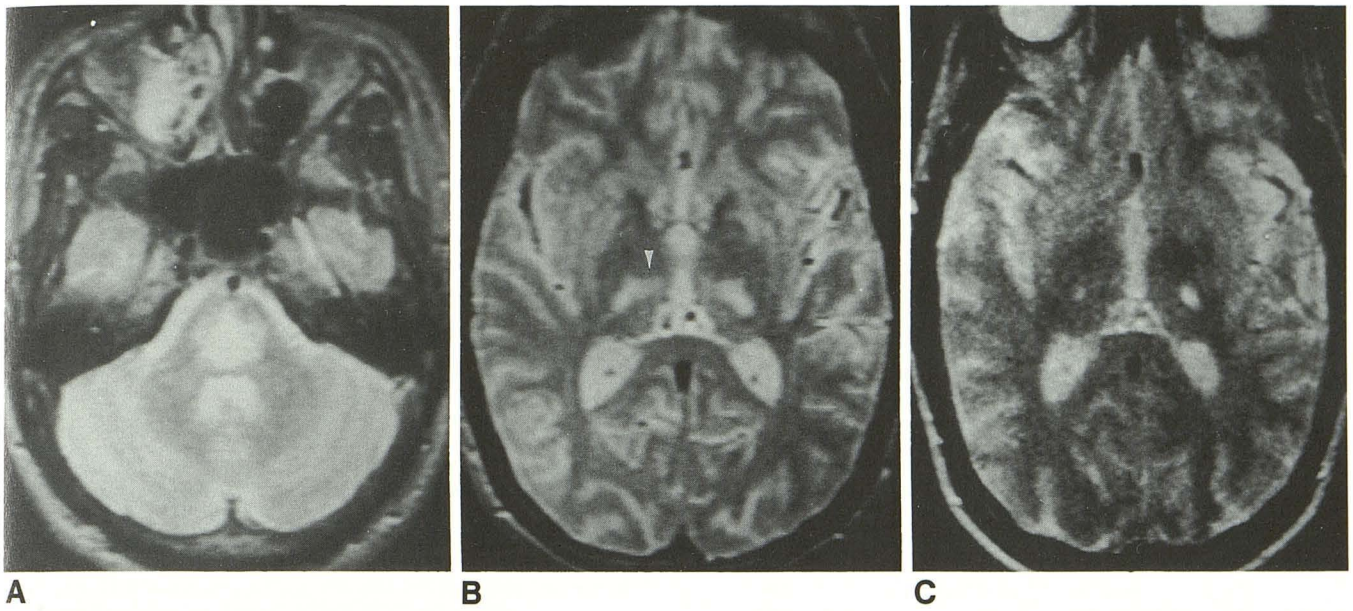

Fig. 2.—Case 3.
A and *B*, Axial T2-weighted MR image (2500/70) on day 17 shows typical central pontine myelinolysis (*A*) and prominent bilateral thalamic lesions consistent with extrapontine myelinolysis (*B*). The medialmost thalamic involvement (*arrowhead* in *B*) at midventral thalamic level corresponds to the myelinated centromedian nucleus (Figs. 3 and 4B).
C, Axial T2-weighted MR image (2000/100) at 2-month follow-up shows decrease in size of thalamic lesions.

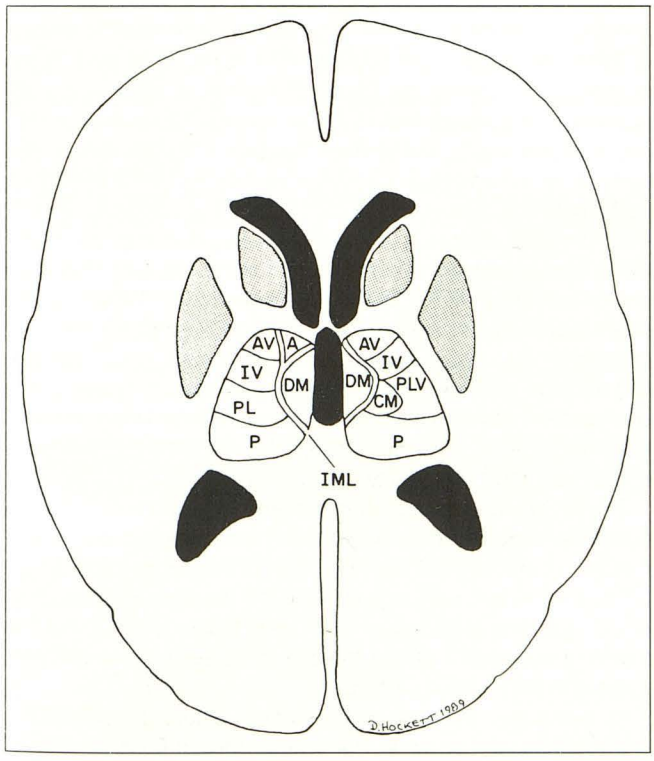

Fig. 3.—Diagrammatic representation of major thalamic nuclei at mid-dorsal thalamic level (portion of diagram to viewer's left) and midventral thalamus (viewer's right). A = anterior nucleus, AV = anterior ventral nucleus, IV = intermediate ventral nucleus, PL = posterior lateral nucleus, P = pulvinar, DM = dorsal medial nucleus, PLV = posterior lateral ventral nucleus, CM = centromedian nucleus, IML = internal medullary lamina.

pattern demonstrated on the T2-weighted MR images, wherein bright symmetric lesions involve the lateral portion of the thalamus with sparing of the pulvinar and medial nuclear regions. Correlation of the MR images (Figs. 1D and 2B) with a schematic representation of the thalamic nuclear groups (Fig. 3) would place the lesions predominantly within the posterior lateral, posterior lateral ventral, intermediate ventral, and centromedian nuclei. The thalamic lesions do not appear to represent contiguous extensions of the pontine lesions even when there is midbrain involvement, as in case 3.

In three previously reported cases of CPM, bilateral thalamic lesions were also identified on CT [9] and MR [6, 7], and the pattern of involvement on the published images showed the same lateral thalamic distribution as in our cases.

There is no proven explanation for the pathogenesis or location of lesions in CPM/EPM, but Norenberg [17] and others [12, 18–20] have noted lesion occurrence within areas of rich gray-white matter apposition. They propose that osmotically induced endothelial changes result in myelinotoxic factors and/or edema derived from gray matter (which has five times the vascularity of white matter). Interestingly, the location of lesion involvement on MR (see Figs. 1D and 2B) parallels the pattern of myelination within the thalami on normal brain specimens stained for myelin (Figs. 4A and 4B). The relatively myelin-poor medial and pulvinar regions are spared. The adjacent heavily myelinated posterior limbs of the internal capsule are relatively unaffected. This observation would support the hypothesis of an important role of gray-white matter admixture in the pathogenesis of EPM/CPM.

The evolution of CPM and EPM has been described on serial CT imaging [10, 21]. Case 2 (Fig. 1) is to our knowledge the first case report in which MR demonstrates very early lesions in the development of CPM/EPM. At postmortem

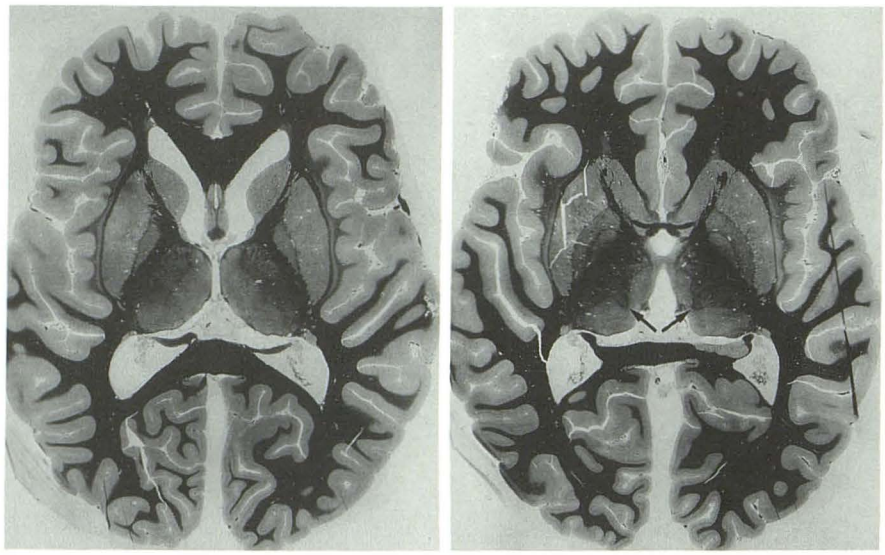

Fig. 4.—Normal brain specimen stained for myelin (Loyez stain).
A, At middorsal thalamic level.
B, At midventral thalamic level. Note the relatively myelin-poor dorsal medial nucleus and pulvinar. The well-myelinated centromedian nucleus (*arrows*) correlates with the medial extent of thalamic lesions in case 3 (Fig. 2B).

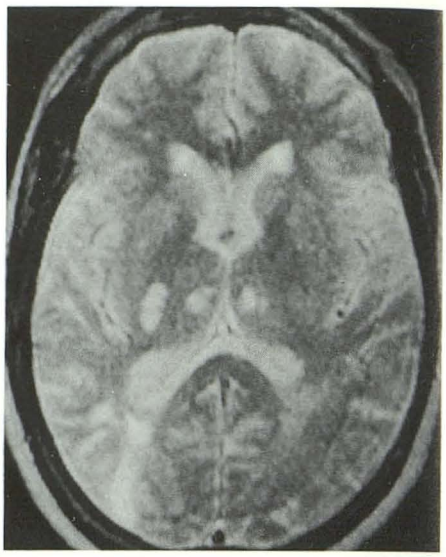

Fig. 5.—Axial T2-weighted MR image (2000/100) shows bilateral paramedian thalamic infarctions. The medial location of these symmetric lesions differentiates this entity from thalamic extrapontine myelinolysis (Fig. 1D). Other infarcts are seen at the right posterior limb internal capsule and right occipital lobe.

examination these early lesions may be seen as small central pontine areas of myelinolysis extending only 2–3 mm on either side of the median raphe [15].

Clinical recovery in CPM and documentation of lesion dimunution by both CT and MR, as demonstrated in case 3, has been reported previously [22–24].

Although contrast enhancement of CPM has been described recently [7], the only case receiving contrast medium in our series (case 1) showed no enhancement.

With respect to differential diagnosis, a review of the literature reveals that the CT or MR finding of bilateral symmetric thalamic lesions is relatively uncommon and many examples are sole case reports or rare metabolic syndromes presenting in infants or children. These include Leigh disease [25], Wilson disease [26, 27], cytoplasmically inherited striatal degeneration [28], Sandhoff disease (GM_2 gangliosidosis) [29], and Krabbe disease [30]. Single case reports of inflammatory processes in children—including measles encephalitis [31], Reye syndrome [32], and acute febrile encephalopathy [33]—have cited symmetric thalamic lesions. Transient thalamic hypodensity was shown on CT following generalized seizures in an adult with lupus erythematosus [34].

Anoxic-hypoxic insults in the neonate can result in symmetric bithalamic and basal ganglia hemorrhage [35, 36]. Near-drowning in young children has also been associated with symmetric thalamic lesions [37]. In cases of EPM in which thalamic lesions are not present, the MR and CT appearance of basal ganglia lesions can be indistinguishable from the changes commonly seen in anoxia. CPM if present can help differentiate the two entities, as the brainstem is usually spared in anoxic-hypoxic insults. Wernicke-Korsakoff syndrome occasionally manifests bilateral symmetric thalamic hypodense lesions on CT [38, 39]. These have involved either the entire thalamus or medial thalamus and should be distinguishable from the "typical" laterally placed thalamic lesions in EPM. Recently, focal hyperintense thalamic lesions at the dorsal medial nuclei on T2-weighted MR images were described in a case of Wernicke syndrome (Donnal JF et al., paper presented at the annual meeting of the American Society of Neuroradiology, Los Angeles, March 1990). Pathologically, neuronal loss is most prominent in the relatively unmyelinated medial thalamus [40]. MR has also documented mamillary body atrophy in alcoholics with classic Wernicke encephalopathy [41]. Clinical differentiation of Wernicke encephalopathy from early CPM/EPM can be difficult, as both entities tend to occur in the same patient population (alcoholics) and the triad of mental status abnormalities, ataxia, and oculomotor abnormalities can closely resemble the presentation of patients with early CPM/EPM. Importantly, Wernicke encephalopathy is treatable with thiamine.

Finally, bilateral paramedian thalamic infarctions (Fig. 5) can occur by occlusion of a single trunk that supplies both paramedian thalamic arteries [42, 43]. Concurrent midbrain or pontine infarction may accompany the thalamic infarcts. This could raise the question of CPM with thalamic EPM, but the medial involvement of the thalami in these infarcts differentiates this entity from CPM/EPM.

In summary, thalamic extrapontine lesions in CPM/EPM characteristically occur in the lateral portion (and centromedian nucleus) of the thalami, paralleling the pattern of myelination. In the proper clinical setting, the MR detection of bilateral symmetric thalamic lesions in association with central pontine or symmetric basal ganglia lesions should facilitate the diagnosis of CPM/EPM.

Addendum

We have recently seen a fourth case of CPM with thalamic EPM in the same pattern as those cases described in this report.

REFERENCES

1. Adams RD, Victor M, Mancall EL. Central pontine myelinolysis. A hitherto undescribed disease occurring in alcoholic and malnourished patients. *Arch Neurol Psychiatry* **1959**;81:154–172
2. Gocht A, Colmant HJ. Central pontine and extrapontine myelinolysis: a report of 58 cases. *Clin Neuropathol* **1987**;6:262–270
3. Morikawa F, Tashiro K, Maruo Y, et al. MR imaging of pontine and extrapontine myelinolysis. *J Comput Assist Tomogr* **1988**;12:446–449
4. Dickoff DJ, Raps M, Yahr MD. Striatal syndrome following hyponatremia and its rapid correction. A manifestation of extrapontine myelinolysis confirmed by magnetic resonance imaging. *Arch Neurol* **1988**;45:112–114
5. Gerard E, Healy ME, Hesselink JR. MR demonstration of mesencephalic lesions in osmotic demyelination syndrome (central pontine myelinolysis). *Neuroradiology* **1987**;29:582–584
6. Rippe DJ, Edwards MK, D'Amour PG, et al. MR imaging of central pontine myelinolysis. *J Comput Assist Tomogr* **1987**;11:724–726
7. Koch KJ, Smith RR. Gd-DTPA enhancement in MR imaging of central pontine myelinolysis. *AJNR* **1989**;10:S58
8. Price DB, Kramer J, Hotson GC, et al. Central pontine myelinolysis: report of a case with distinctive appearance on MR imaging. *AJNR* **1987**;8: 576–577
9. Thompson DS, Hutton T, Stears JC, et al. Computerized tomography in the diagnosis of central and extrapontine myelinolysis. *Arch Neurol* **1981**;38:243–246
10. Hazratji SMA, Kim RC, Lee SH, et al. Evolution of pontine and extrapontine myelinolysis. *J Comput Assist Tomogr* **1983**;7:356–361
11. Kalnins RM, Berkovic SF, Bladin PF. Central pontine myelinolysis with widespread extrapontine lesions: a report of two cases. *Clin Exp Neurol* **1984**;20:189–202
12. Okeda R, Kitano M, Sawabe M, et al. Distribution of demyelinating lesions in pontine and extrapontine myelinolysis—three autopsy cases including one case devoid of central pontine myelinolysis. *Acta Neuropathol (Berl)* **1986**;69:259–266
13. Boon AP, Potter AE. Extensive extrapontine and central pontine myelinolysis associated with correction of profound hyponatremia. *Neuropathol Appl Neurobiol* **1987**;13:1–9
14. Thompson AJ, Brown MM, Swash M, et al. Autopsy validation of MRI in central pontine myelinolysis. *Neuroradiology* **1988**;30:175–177
15. Wright DG, Laureno R, Victor M. Pontine and extrapontine myelinolysis. *Brain* **1979**;102:361–385
16. Miller GM, Baker HL, Okazaki H, et al. Central pontine myelinolysis and its imitators: MR findings. *Radiology* **1988**;168:795–802
17. Norenberg MD. A hypothesis of osmotic endothelial injury. A pathogenetic mechanism in central pontine myelinolysis. *Arch Neurol* **1983**;40:66–69
18. Messert B, Orrison WW, Hawkins MJ, et al. Central pontine myelinolysis. Consideration on etiology, diagnosis, and treatment. *Neurology* **1979**; 29:147–160
19. Goldman JE, Horoupian DS. Demyelination of the lateral geniculate nucleus in central pontine myelinolysis. *Ann Neurol* **1981**;9:185–189
20. Oda Y, Okada Y, Nakanishi I, et al. Central pontine myelinolysis with extrapontine lesions. *Acta Pathol Jpn* **1984**;34:403–410
21. Rosenbloom S, Buchholz D, Kumar AJ, et al. Evolution of central pontine myelinolysis on CT. *AJNR* **1984**;5:110–112
22. Gerber O, Geller M, Stiller J, et al. Central pontine myelinolysis. Resolution shown by computed tomography. *Arch Neurol* **1983**;40:116–118
23. Schroth G. Clinical and CT confirmed recovery from central pontine myelinolysis. *Neuroradiology* **1984**;26:149–151
24. Ragland RL, Duffis AW, Gendelman S, et al. Central pontine myelinolysis with clinical recovery: MR documentation. *J Comput Assist Tomogr* **1989**;13:316–318
25. Schwartz WJ, Hutchison HT, Berg BO. Computed tomography subacute necrotizing encephalomyelopathy (Leigh disease). *Ann Neurol* **1981**;3: 268–271
26. Lawler GA, Pennock JM, Steiner RE, et al. Nuclear magnetic resonance (NMR) imaging in Wilson disease. *J Comput Assist Tomogr* **1983**;7:18
27. Starosta-Rubinstein S, Young AB, Kluin K, et al. Clinical assessment of 31 patients with Wilson's disease. Correlations with structural changes on magnetic resonance imaging. *Arch Neurol* **1987**;44:365–370
28. Seidenwurm D, Novotny E, Marshall W, et al. MR and CT in cytoplasmically inherited striatal degeneration. *AJNR* **1986**;7:629–632
29. Stalker HP, Han BK. Thalamic hyperdensity: a previously unreported sign of Sandhoff disease. *AJNR* **1989**;10:S82
30. Baram TZ, Goldman AM, Percy AK. Krabbe disease: specific MRI and CT findings. *Neurology* **1986**;36:111–115
31. Ochi J, Okuno T, Uenoyama Y, et al. Symmetrical low density areas in bilateral thalami in an infant with measles encephalitis. *Comput Radiol* **1986**;10:137–139
32. Hino T, Sai H, Morikawa R, et al. A case of clinical Reye syndrome presenting characteristic CT change. *No To Hattatsu* **1984**;16:210–217
33. Tateno A, Sakai K, Sakai S, et al. Computed tomography of bilateral thalamic hypodensity in acute encephalopathy. *J Comput Assist Tomogr* **1988**;12:637–639
34. Vern BA, Butler M. Transient thalamic hypodensity in lupus erythematosus with generalized seizures. *Neurology* **1983**;33:1081–1083
35. Kotagal S, Toce SS, Kotagal P, et al. Symmetric bithalamic and striatal hemorrhage following perinatal hypoxia in a term infant. *J Comput Assist Tomogr* **1983**;7:353–355
36. Kreusser KL, Schmidt RE, Shackelford GD, et al. Value of ultrasound for identification of acute hemorrhagic necrosis of thalamus and basal ganglia in an asphyxiated term infant. *Ann Neurol* **1984**;16:361–363
37. Taylor SB, Quencer RM, Holzman BH, et al. Central nervous system anoxic-ischemic insult in children due to near drowning. *Radiology* **1985**;156:641–646
38. McDowell JR, LeBlanc HJ. Computed tomographic findings in Wernicke-Korsakoff syndrome. *Arch Neurol* **1984**;41:453–454
39. Mensing JWA, Hoogland PH, Slooff JL. Computed tomography in the diagnosis of Wernicke's encephalopathy: a radiological neuropathological correlation. *Ann Neurol* **1984**;16:363–365
40. Charness ME, Simon RP, Greenberg DA. Ethanol and the nervous system. *N Engl J Med* **1989**;321:442–453
41. Charness ME, DeLaPaz RL. Mamillary body atrophy in Wernicke's encephalopathy: antemortem identification using magnetic resonance imaging. *Ann Neurol* **1987**;22:595–600
42. Gerber O, Gudesblatt M. Bilateral paramedian thalamic infarctions: a CT study. *Neuroradiology* **1986**;28:128–131
43. Castaigne P, Lhermitte F, Buge A, et al. Paramedian thalamic and midbrain infarcts: clinical and neuropathological study. *Ann Neurol* **1981**;10: 127–148